

Dielectric Relaxation and Ferroelectric Imprint

Herbert Kliem
Institute of Electrical Engineering Physics
Saarland University
Germany
h.kliem@mx.uni-saarland.de

Abstract—The term imprint is generally used for a special kind of a reversible change in the ferroelectric state. It refers to a time dependent development of the material's resistance against polarization reversal. At the example of P(VDF-TrFE) it is shown that if polarized to the remanent polarization and under a switched off external field the **coercive field of the sample's hysteresis loop increases** in time, the ferroelectric switching time increases as well, the remanent polarization decreases, and the **small signal ac capacitance decreases** also. All four effects exhibit a linear behavior on a logarithmic time scale, i.e. they are proportional to $\log t_w$, with t_w as the waiting time after switching off the external field. A model is developed which relates the four observations. The model is based on a feedback effect between a crystalline phase where the ferroelectric switching takes place and an amorphous or disordered phase with a relaxational polarization response.

I. INTRODUCTION

The term imprint in ferroelectrics summarizes the effect of a time dependent resistance of the material against ferroelectric polarization reversal. Consider a ferroelectric polarized to the remanent polarization. The applied field E_a is switched off at time $t = 0$. Waiting a time t_w in this state results in a coercive field E_c which is higher than the field E_c found in continuous runs through the hysteresis loop. The longer t_w is, the higher is the field necessary to reverse the polarization. More exactly, there is a logarithmic dependence $E_c(t_w)$. Qualitatively the same observation can be made with respect to the system's switching time t_s . Applying a step like field larger than E_c against the polarization direction the polarization will be reversed but the switching time t_s increases as the waiting time t_w increases. Also here we find a logarithmic dependence $t_s(t_w)$, see below. This behavior is not restricted to a polymer like poly(vinylidene fluoride / trifluoroethylene) [1] [2], P(VDF-TrFE), but is also found in ceramic materials like lead zirconium titanate, PZT, [3], [4], bariumtitanate, BaTiO₃ [5], or bismuth sodium titanate, BNT [6]. It is obvious that imprint worsens the applicability of ferroelectrics for instance as memories since the writing speed, i.e. the polarization reversal time, is affected by the time elapsed after poling. For the case of P(VDF-TrFE) the following observations are made additionally: When a field is applied to switch the ferroelectric, first a short term switching event is observed usually during the first milliseconds. Afterwards a slow long term increase of the polarization lasting over hundreds up to thousands of seconds is found. Switching off the field, the remanent polarization decays slowly for again thousands of seconds. Both long term events follow a logarithmic law in time. An indirect way to observe the imprint effect is the measurement of the small signal ac capacitance $C_{ac}(E_a=0)$ in the remanent state. When the loop

is shifted towards higher fields $C_{ac}(E_a=0)$ decreases in time. Also $C_{ac}(t_w)$ follows a logarithmic time dependence. It is the aim of this contribution to develop a model which links the four experimental observations.

II. THE EXPERIMENTS

Samples were prepared as metal-P(VDF-TrFE)-metal structures by a standard spin coating technique followed by an annealing process at elevated temperatures for the ferroelectric layer and subsequent thermal evaporation of aluminum as electrode [1], [7]. The thickness of the ferroelectric is between 67 nm and 935 nm. To gain a well defined start position for the imprint measurements a deaging procedure was applied described in [1]. After the deaging process the hysteresis loop of the sample's displacement vs. applied voltage is measured. The measurement stops in the negative remanent polarization.

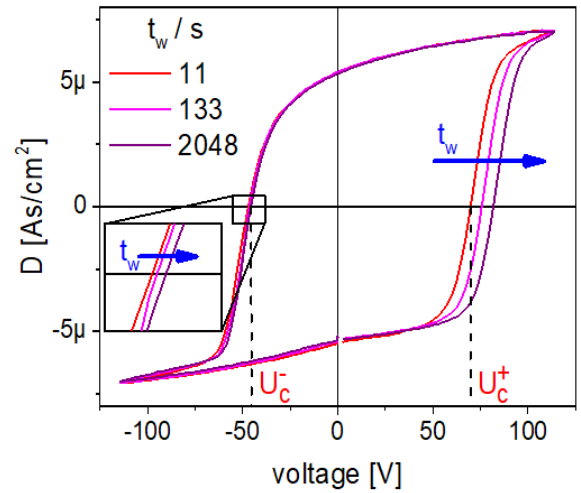


Fig. 1 The hysteresis loops after different waiting times t_w . For an applied voltage $U = 0$ V the loops are centered with respect to the remanent polarization. Sample thickness: 935 nm.

After different waiting times t_w in the negative remanent polarization state the loop is measured again. A pronounced shift of the coercive voltage U_c^+ is observed which increases with t_w (Fig. 1). However, the shift in U_c^- is noticeably smaller.

Fig. 2 presents the temporal development of the coercive voltage for different sample thicknesses. This figure demonstrates that imprint is **independent** of the sample **thickness** and therefore **it is a volume effect**.

The mean shift is described by

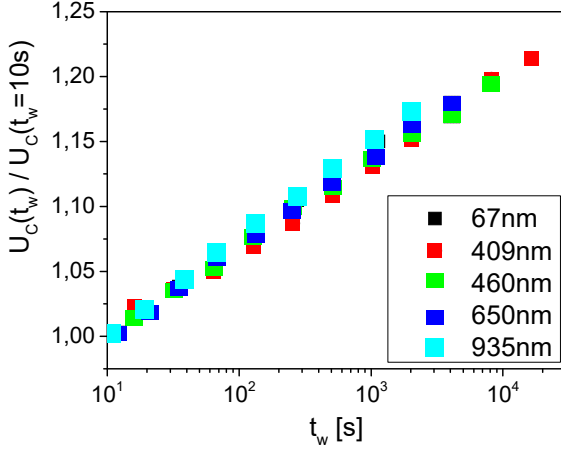


Fig. 2. The normalized shift of the coercive voltage with waiting time t_w is independent of the sample thickness.

$$U_c(t_w) = \frac{U_c^+ + U_c^-}{2} = U_0 + U_1 \log \frac{t_w}{s} \quad (1)$$

Next the switching of the polarization is measured after different times t_w of waiting in the negative remanent polarization state, Fig. 3. It is obvious that the switching to the positive polarization is slowed down with the waiting time.

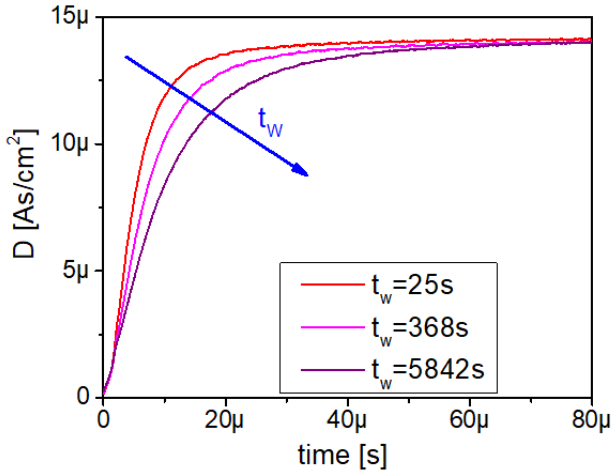


Fig. 3. Switching events after different waiting times. Sample thickness 935 nm, applied field $E_a = 130$ MV/m

Fig. 4 depicts the ferroelectric system's switching time t_s for different waiting times t_w and sample thicknesses. The change in t_s is independent of the sample thickness. Similar to Fig. 2 we find an increase of t_s with $\log t_w$.

Also this experiment points towards a volume effect for an interpretation of the imprint. While for the observation of $E_c(t_w)$ and $t_s(t_w)$ the ferroelectric state must be perturbed the measurement of the small signal ac capacitance $C_{ac}(t_w, E_a = 0)$, i.e. the capacitance in the remanent polarization state, preserves the polarization. When the hysteresis $P(E)$ is shifted on the E-axis towards positive E, the slope of the hysteresis at $E_a = 0$ decreases. For low frequencies the slope is proportional to the small signal ac capacitance. This change in the capacitance is depicted in Fig. 5 for different sample thicknesses. A logarithmic law is found for all

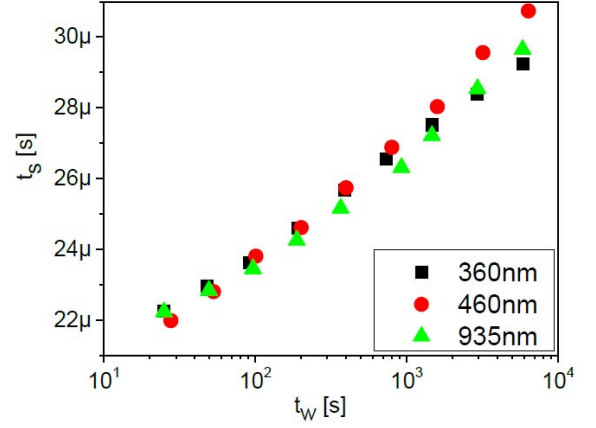


Fig. 4. The system's switching time t_s in dependence of t_w with the sample thickness as parameter. $E_a = 130$ MV/m.

thicknesses

$$C_{ac}(t_w) = C_0 - C_1 \log \frac{t_w}{100s} \quad (2)$$

The curves are normalized to $C_{ac}(t=100s)$.

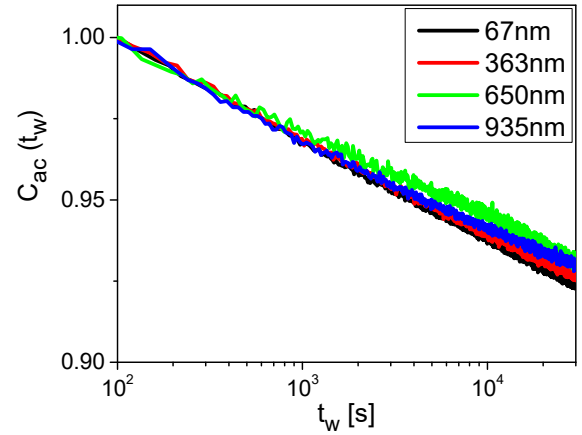


Fig. 5. The time dependent normalized capacitance for $f=10$ kHz for different thicknesses.

The fading of the remanent polarization after a switching event, also known as aging of the ferroelectric state, is measured after a switching pulse of 10s duration, Fig. 6. The decay of the remanent polarization is measured by the short circuit current. The current decreases almost with a power law

$$j \cong A \cdot t^{-\alpha}, \alpha \approx 1 \quad (3)$$

Integration yields the decay of remanent polarization

$$P_r(t) = P_r(t_0) - A \int_{t_0}^t (t')^{-\alpha} dt' = P_r(t_0) - B \log \frac{t}{t_0} \quad (4)$$

Thus we get the same time dependence as found for the coercive field, the switching time, and the capacitance. For different thicknesses the currents have the same magnitude and follow over more than 10^4 s the power law.

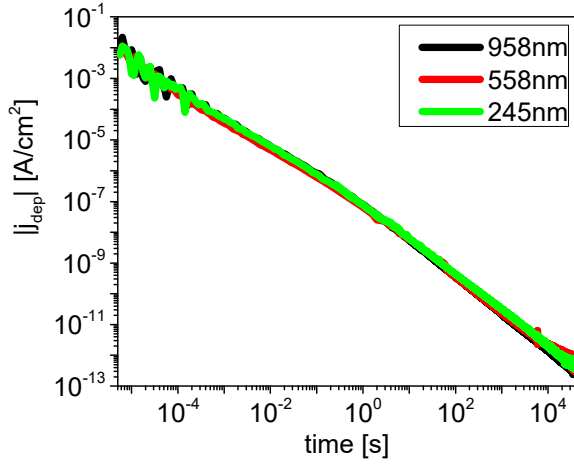


Fig. 6. The depolarization currents after a switching pulse of 10s duration for different sample thicknesses. The voltage applied before was always 1.8 times the average coercive voltage ($E_c = \text{const}$).

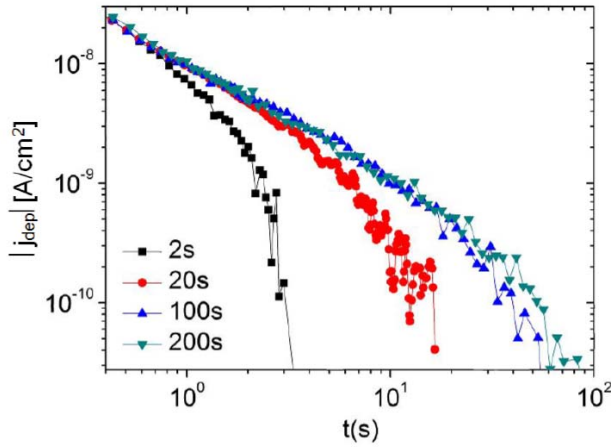


Fig. 7. Non switching pulses of different lengths are applied (2s to 200s). The depolarization current indicates LTI behaviour.

This demonstrates that after a switching event the system can not be described as a linear time invariant (LTI) system. For a LTI system composed of different relaxation processes with a distribution of relaxation times the depolarization current should decrease faster than $t^{-\alpha}$ for times longer than the charging pulse duration i.e. after 10s in the present case. This is because in a LTI system only those relaxation processes can contribute to the depolarization currents which are excited during the charging pulse, i.e. only processes with relaxation times up to 10s.

In contrast, if the applied voltage is smaller than the coercive voltage no switching appears and the sample behaves like a LTI system. This is demonstrated in Fig. 7. The depolarization current falls down faster than t^{-1} for times longer than the charging pulse [8].

A similar result was found earlier [9] using the field reversal experiment suggested by T. Guo and W. Guo [10]. It was shown that the system can be looked at as non-LTI in the ferroelectric state, and that it behaves like LTI in the paraelectric state.

This observation of a LTI system after a non switching pulse and the observation of a non-LTI system after a

switching pulse yields the key for the understanding of the imprint effect.

III. THE MODEL

In P(VDF-TrFE) an amorphous and a crystalline phase exist in parallel [11]. In the crystalline phase the elementary permanent dipoles or charges responsible for the ferroelectric polarization are found on regular lattice sites. They are assumed to fluctuate in double well potentials (Fig. 8). All of them have identical properties, i.e. activation energy W_0 and distance R between the wells. Due to further charges in the crystallite the double wells can have an intrinsic asymmetry V . The dipoles/charges align parallel or anti-parallel to the direction of the field. Therefore they can give rise to a specific reaction field at the location of the dipole sites, the Weiss-field which is proportional to the polarization of the sample. This field is analogous to the Lorentz field for induced dipoles. Then the local field at the dipoles responsible for the ferroelectric polarization is the sum of the applied field E_a and the Weiss-field $E_w = \beta P$ with β as a coupling constant

$$E_{loc} = E_a + \beta P \quad (5)$$

The validity of eqn.(5) was confirmed in [12] with a microscopic simulation.

In the amorphous phase dipoles and/or charges fluctuate also in double well potentials but their axes are distributed in random directions. Also the distances between the wells may be distributed described by the pair distribution function of atoms related to the amorphous state. With a distribution of distances a distribution of barrier heights can be expected also. Since the distances to neighbored charges outside the double wells are distributed in the amorphous state the double well potentials here can have an intrinsic asymmetry too. Due to the randomness of the amorphous phase a feedback field as present in the crystalline state can not exist.

The basic element for the physical interpretation of the imprint effect is therefore the asymmetric double well potential where charges/dipoles can fluctuate between two minima. There can exist left and right asymmetries (Fig. 8).

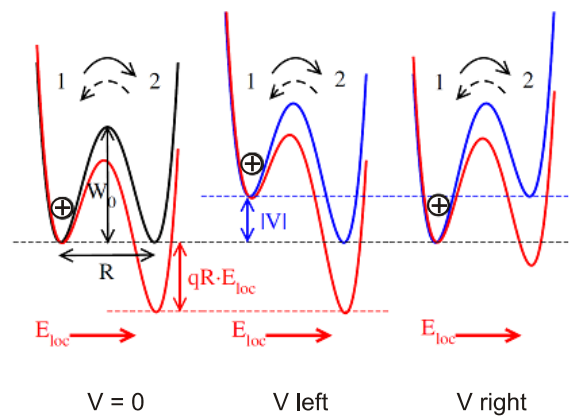


Fig. 8. The double well potentials. Due to charges outside the double wells an intrinsic asymmetry V may exist. This asymmetry is shifted by $qR \cdot E_{loc}$ due to the local field described with eqn.(5). Charges fluctuate thermally activated or by phonon assisted tunneling in between the double wells.

The total number n of charges in the double wells is constant ($n_{1,2}$: charges in well 1,2)

$$n = n_1 + n_2 \quad (6)$$

In the crystalline phase a feedback loop for the polarization P exists resulting in the ferroelectric state while in the amorphous phase the dipoles relax with negligible interactions ($\beta=0$). After a perturbation the charges redistribute following first order rate equations with the transition probabilities w_{12} and w_{21}

$$\frac{\partial n_1}{\partial t} = -w_{12}n_1 + w_{21}n_2 = -\frac{\partial n_2}{\partial t} \quad (7)$$

The local field E_{loc} shifts the asymmetry V to $qRE_{loc} \pm V$ and we find for a thermal activation (τ_0 : reciprocal phononfrequency) of single charges

$$w_{12} = \frac{1}{\tau_0} \exp \left[-\frac{W_0 - (qRE_{loc} \pm V)/2}{kT} \right] \quad (8)$$

$$w_{21} = \frac{1}{\tau_0} \exp \left[-\frac{W_0 + (qRE_{loc} \pm V)/2}{kT} \right]$$

With these transition probabilities the responses in the amorphous and in the crystalline phase can be calculated. The polarization $P(t)$ is the difference of the occupation densities n_2 and n_1 multiplied with the dipole moment p

$$P(t) = (n_2(t) - n_1(t))p \quad (9)$$

For the single charges the dipole moment is $p = qR/2$.

We find with (7), (8), (9) and $P_{sat} = (n_1 + n_2)p$

$$\tau \frac{\partial P(t)}{\partial t} + P(t) = P_{sat} \tanh \left(\frac{qRE_{loc} \pm V}{2kT} \right) \quad (10)$$

with the system's time constant

$$\tau = \frac{1}{w_{12} + w_{21}} = \frac{\tau_0}{2} \exp \left(\frac{W_0}{kT} \right) / \cosh \left(\frac{qRE_{loc} \pm V}{2kT} \right) \quad (11)$$

A. The relaxational response in the amorphous phase

Due to the disordered structure of the amorphous phase one can expect a distribution of distances R for the double wells. The distribution of R causes a distribution of barrier heights W_0 between the wells. It is deduced in [13] for the case of amorphous aluminum oxide how W_0 can depend on R . A feedback field βP does not exist in the random structure. Thus we have $E_{loc} = E_a$. The directions of the double wells are distributed in space. For a rigorous treatment an integration over all angles was carried out in [14]. For a qualitative analysis it is assumed that the axes are only parallel or antiparallel to the applied field, i.e. V has to be counted only positive or negative. For $V=0$ the equilibrium polarization $P(E_a)$, the right side of eqn.(10), is the tanh-curve. For $\pm V \neq 0$ the curve is shifted along the negative and positive E_a -axis. Both contributions superimpose and the response becomes strongly nonlinear. From (10) it follows for a distance R

$$P(t \rightarrow \infty) = P_{sat} \left[\frac{1}{2} \tanh \frac{qRE_a + V}{2kT} + \frac{1}{2} \tanh \frac{qRE_a - V}{2kT} \right] \quad (12)$$

This is sketched with Fig. 9.

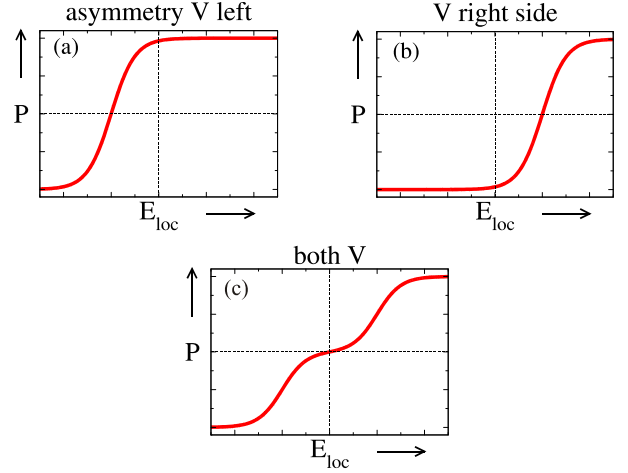


Fig. 9. Left and right handed asymmetries superimpose. For non-interacting dipoles: $E_{loc} = E_a$. Simplification: R parallel to E_a .

Fig. 10 shows the depolarization currents at a constant time of 10s after switching off the field, for a 69nm thick sample. The currents are nonlinear in the non-switching region and saturate in higher fields. The data points are fitted using eqn.(12) with $R=0.2nm$, $V=52meV$ and E_a the field applied before [8]. Thus the nonlinearity yields the order of the distance between the wells in the amorphous phase.

The dynamic response in the time and frequency domain is related to the distribution density function $h(R)$ of distances R and/or a distribution of the barrier heights W_0 . W_0 can be related to R . The detailed derivation of the time and frequency response in relation to $h(R)$ is given in [13, 14]. An abbreviated calculation is delivered here.

Let W_0 be the leading distributed term. In the small signal response we find with eqn. (11) for the relaxation

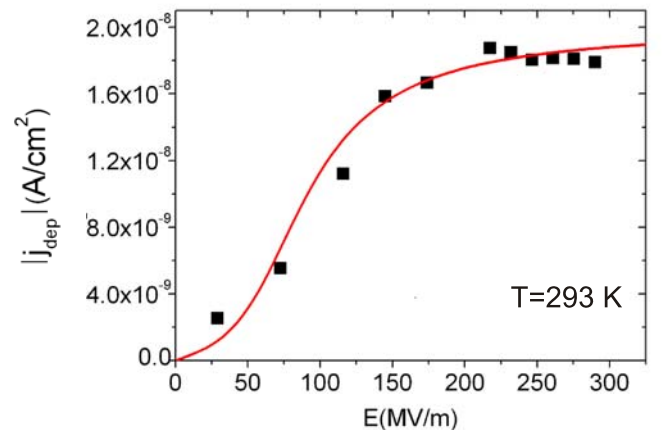


Fig.10. The depolarization currents at 10s after switching off the field at room temperature. Sample thickness 69nm.

frequencies $\nu = 1/\tau$

$$\nu = \nu_0 \exp \left\{ -\frac{W_0}{kT} \right\} \quad (13)$$

For a distribution of W_0 between 0.1eV and 1eV a distribution of ν over more than 10 decades at room temperature results. An even broader distribution can be expected for a phonon assisted tunneling process approximating for a rectangular barrier

$$\nu = \nu_0 \exp\{-c\sqrt{W_0}R\} \quad (14)$$

and an increase of W_0 with R (c : a constant). A discrimination between tunneling and thermal activation was carried out in [13, 14].

Eqns. (13) and (14) have the form

$$\nu = \nu_0 \exp\{-\Delta\} \quad (15)$$

Let $f(\nu)$ be the distribution density function of ν . Then we find for the processes with relaxation frequencies ν in between ν and $\nu+d\nu$

$$dP = P(t \rightarrow \infty) f(\nu) d\nu \quad (16)$$

Eqn.(10) now takes the form

$$\frac{1}{\nu} \frac{\partial}{\partial t} dP(t) + dP(t) = P(t \rightarrow \infty) f(\nu) d\nu \quad (17)$$

with the solution

$$dP(t) = P(t \rightarrow \infty) f(\nu) d\nu (1 - \exp\{-t \cdot \nu\}) \quad (18)$$

The (de)polarization current density is the time derivative

$$dj(t) = \frac{\partial}{\partial t} dP(t) = P(t \rightarrow \infty) \nu f(\nu) \exp\{-t \cdot \nu\} d\nu \quad (19)$$

Thus we find for $j(t)$ a Laplace-transform of $\nu f(\nu)$

$$j(t) = P(t \rightarrow \infty) \int_0^\infty \nu f(\nu) \exp\{-t \cdot \nu\} d\nu \quad (20)$$

With $g(\Delta)$ as the distribution density function of Δ and

$$f(\nu) d\nu = g(\Delta) d\Delta \quad (21)$$

we get for $g(\Delta) = \text{const}$ [15]

$$j(t) = A \cdot t^{-1} \quad (22)$$

within the limits predicted by the limits of $g(\Delta)$. This result is obtained for parallel processes relaxing independently. Fig. 11 depicts the calculated depolarization currents flowing after different lengths of charging pulses [16]. This result can be directly compared to Fig.7 where non switching pulses of different lengths were applied. We see that the relaxational response yields a LTI system if it is not perturbed by a switching event of the ferroelectric phase.

B. The ferroelectric response of the crystalline phase

For the description of the ferroelectricity in the crystalline phase the Weiss-model [17] shall be used. The Weiss-model is applied to the double well potential, Fig. 8. As explained above, the Weiss-field is a feedback field βP_{fe} proportional to the polarization of the sample which acts only at the location of the dipoles on their crystallographic sites similar to the Lorentz field. With eqn.(5) we get a

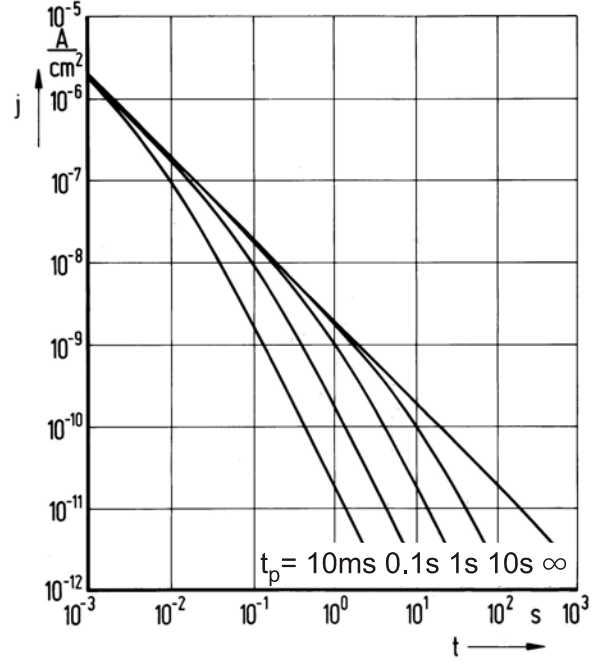


Fig.11. Depolarization currents in a LTI system calculated for different lengths t_p of the charging pulse. Experiment: see Fig.7

feedback loop

$$E_a \rightarrow E_{loc} \rightarrow P_{fe} \quad (23)$$

The subscript "fe" denotes the ferroelectric polarization.

The fluctuation of the dipoles/charges in the double wells is still described with eqn. (8) resulting in the differential eqn.(10) for the time dependence of the polarization. The same formulation is found for the time constant defined in eqn. (11). In contrast to the amorphous phase, now for E_{loc} the interaction has to be taken into account with eqn. (5). Thus we have

$$P_{fe}(t \rightarrow \infty) = P_{sat,fe} \left[\frac{1}{2} \tanh \frac{qR(E_a + \beta P_{fe}) + V}{2kT} + \frac{1}{2} \tanh \frac{qR(E_a + \beta P_{fe}) - V}{2kT} \right] \quad (24)$$

The static polarization is computed using (10) and (24) by solving the nonlinear equation

$$P_{fe}(t \rightarrow \infty) - P_{fe}(t) = \tau \frac{\partial}{\partial t} P_{fe}(t) = 0 \quad (25)$$

Typical parameters used for the computation are: $p = 7.4 \cdot 10^{-22} \mu\text{Ccm}$, $n = 1.6 \cdot 10^{22} \text{cm}^{-3}$, $W_0 = 0.25\text{eV}$, $\tau_0 = 10^{-11}\text{s}$, $\beta = 0.05/\epsilon_0$, $V = 0$. The result is plotted in Fig. 12 [18].

We find a spontaneous polarization for $T < T_C$, the Curie temperature, with a second order phase transition. T_C is proportional to the coupling constant β . For $V=0$ we find

$$T_C = \frac{np^2}{k} \beta \quad (26)$$

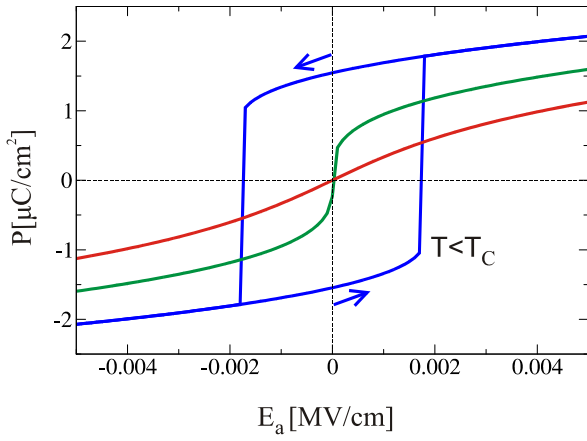


Fig.12. The hysteresis loop of the polarization calculated with the extended Weiss model vanishes at T_C , blue: $T < T_C$, green: $T = T_C$, red: $T > T_C$

It was deduced in [19] that a first order transition with a double loop of the polarization close to T_C appears if the piezoeffect is taken into account. Depending on the asymmetry V and on the interaction strength β the system exhibits ferroelectric or relaxor properties. Also, for $V \neq 0$ we find a double loop close to T_C . High dielectric permittivities in a broad temperature range and a Vogel-Fulcher law for the activation energies could be described combining the asymmetric double well potential model with the Weiss-field theory [12].

C. A model for the imprint

By an interaction between the relaxational response and the ferroelectric response the imprint can be described. Consider the crystalline ferroelectric phase is embedded in the amorphous relaxational phase, Fig. 13a. Applying a field smaller than the coercive field leaves the crystalline phase unaffected. The amorphous phase reacts with the relaxational polarization like a LTI-system. The individual dipoles are aligned in the field and relax back after switching off the field. Next, the applied field exceeds the ferroelectric coercive field and is switched off after a certain duration. Then the ferroelectric polarization is reversed and the stray field of the ferroelectric phase causes an antiparallel alignment of the relaxational dipoles (Fig. 13.a). Now the relaxational current as reaction of the amorphous phase has the same direction as the depolarization current in the LTI system. The process of antiparallel alignment is only dependent on the switched ferroelectric polarization. It does not depend upon the field strength and upon the duration of the field applied before. The whole system reacts as a non-LTI system. While the relaxational dipoles align in antiparallel direction to the ferroelectric dipoles they create a reaction field in the ferroelectric crystal which is a continuous field E_{rel} in the direction of the local fields, i.e. in the direction of the ferroelectric polarization.

In this way the ferroelectric polarization is stabilized Fig. 13b. The field lines of the amorphous phase's dipoles partly end up at the electrodes and partly they form closed loops through the crystalline phase denoted with $E_{rel}(t_w)$. Since the relaxational polarization aligns antiparallel to the ferroelectric one the total polarization measured at the electrodes is decreased in time. The field E_{rel} increases in time with increasing relaxational polarization. The elapsing

time is identical with the waiting time t_w described in section II. Using eqn. (22) $E_{rel}(t_w)$ is approximated by

$$\begin{aligned} E_{rel}(t_w) &= \text{const} \int_{t_0}^{t_w} j_{dep}(t') dt' \\ &= \text{const} A \log \frac{t_w}{t_0} \end{aligned} \quad (27)$$

The field $E_{rel}(t_w)$ should be looked at as an average effective field. The value of "const" in eqn.(27) could be calculated when the geometries of crystal phase and amorphous phase are known. The field $E_{rel}(t_w)$ causes at the double well potentials in the ferroelectric phase an additional asymmetry $\Delta V(t_w)$ which has for both left and right asymmetries V the same direction. The effect of $\Delta V(t_w)$ is to shift one well against the other and to stabilize the polarization (Fig. 13b). Then, a higher field E_a is necessary to compensate the influence of $\Delta V(t_w)$ and to switch the crystal. Thus the hysteresis loop is moved along the E_a -axis.

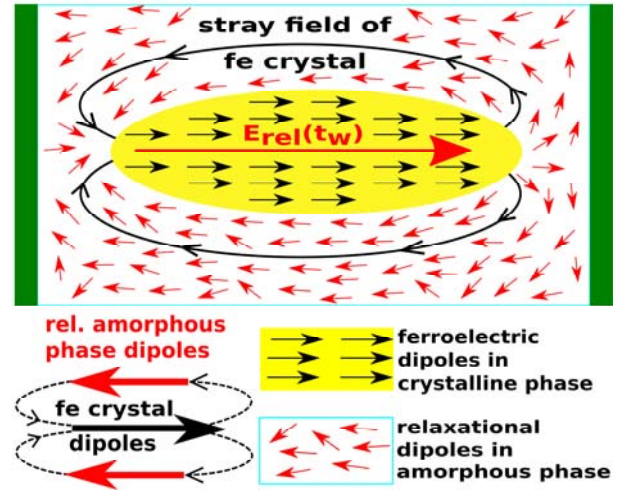


Fig.13a. The ferroelectric crystal generates a stray field which aligns the dipoles/charges in the amorphous phase. The fields of these relaxational dipoles/charges sum up to a time dependent mean field $E_{rel}(t_w)$ which stabilizes in turn the ferroelectric state.

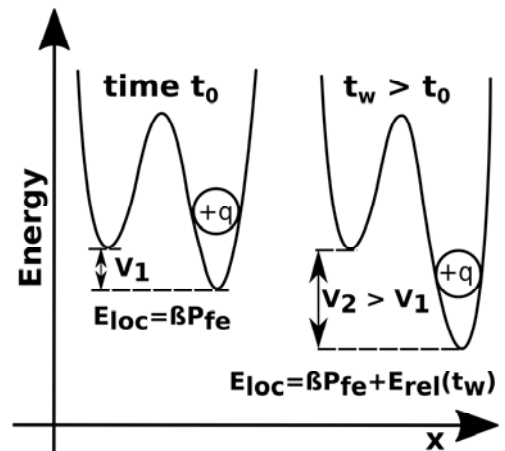


Fig.13b. After the ferroelectric switching event, completed at time t_0 , the asymmetry V at the double wells of the ferroelectric dipoles increases in time due to $E_{rel}(t_w)$.

Then, the local field consists of the Weiss field evoked in the crystalline phase, the relaxation field stimulated in the amorphous phase and the applied field. With

$$\Delta V(t_w) = qRE_{rel}(t_w) = \text{const} \log \frac{t_w}{t_0} \quad (28)$$

we get for the transition probabilities

$$w_{12} = \frac{1}{\tau_0} \exp \left[-\frac{W_0 - (qRE_{loc} \pm V)/2 - \Delta V(t_w)/2}{kT} \right] \quad (29)$$

$$w_{21} = \frac{1}{\tau_0} \exp \left[-\frac{W_0 + (qRE_{loc} \pm V)/2 - \Delta V(t_w)/2}{kT} \right]$$

Using the same algorithm as before we can now compute the hysteresis loops (Fig. 14a) in dependence of the waiting time t_w in the negative remanent polarization state. The loops are shifted to a higher voltage by equal amounts of ΔU_c^+ and ΔU_c^- . In the experiment ΔU_c^- was smaller than ΔU_c^+ . This is due to the fact that by a run through the hysteresis curve fast responding charges/dipoles of the amorphous phase are reverted resulting in a change of E_{rel} . This is not considered in the model and results in the smaller change of U_c^- compared to U_c^+ . Fig. 14b presents the shift of the hysteresis loops with $\log t_w/t_0$ calculated from

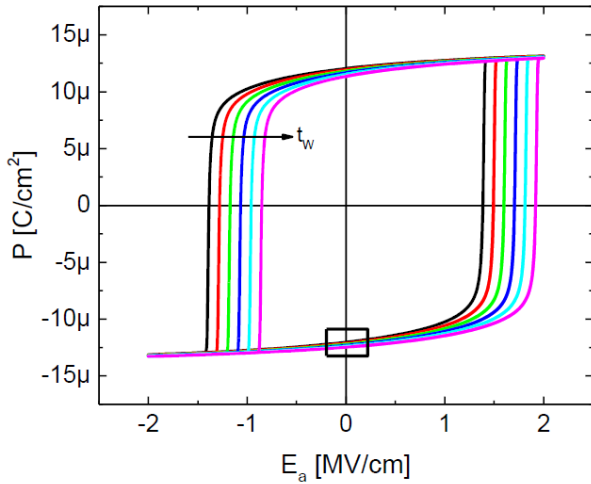


Fig.14 a. The calculated hysteresis curves for different waiting times t_w , experiment: Fig. 1. The asymmetry is 0.01 eV.

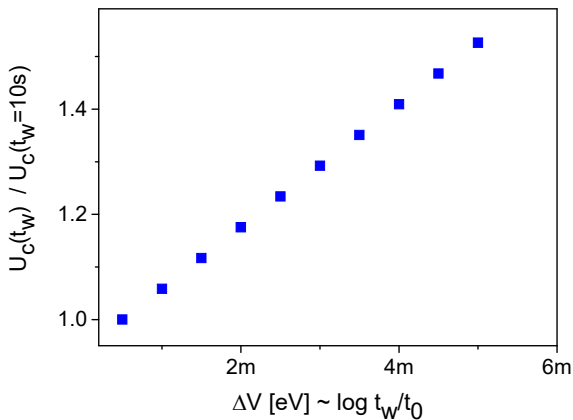


Fig. 14 b. The shift of the hysteresis with $\log t_w$, experiment: Fig. 2

the model. The corresponding experiment is shown in Fig. 2.

Next the system's switching transients in dependence of the waiting time (Fig. 15a) are computed. We find a pronounced increase of the switching time t_s with increasing waiting time t_w as observed in the experiment Fig. 3. In Fig. 15b t_s is plotted versus $\log t_w$. The corresponding experiment is depicted in Fig. 4.

When the loop is moved along the E_a -axis the slope of the loop at $E_a = 0$ changes. With Fig. 16a the small box of Fig. 14a is enlarged showing the decrease of the loop's slope with the waiting time t_w . This slope is apart from the high frequency capacitance proportional to the small field capacitance of the sample at $E_a = 0$ and is easily derived by (Fig. 16b)

$$C_{ac} = \text{const} \frac{\Delta P}{\Delta E_a} \bigg|_{E_a=0, \Delta E_a \rightarrow 0} \quad (30)$$

For the small signal case with $\Delta E_a \rightarrow 0$ the static capacitance is approximately proportional to the small signal ac capacitance (Fig. 5) at a constant frequency.

Thus the model describes correctly the experimentally observed trends.

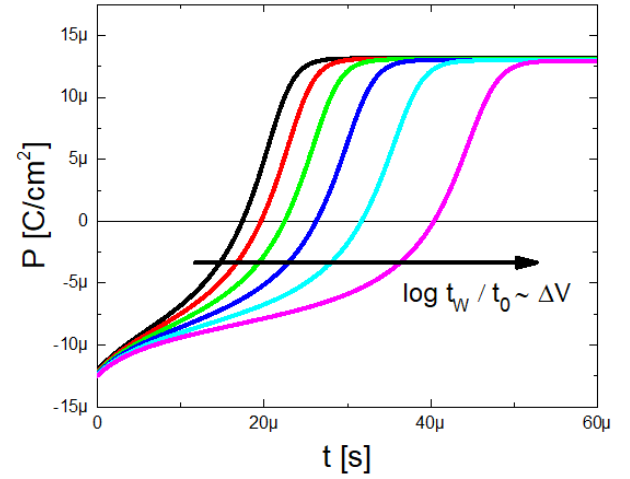


Fig.15a. The calculated switching transients for different waiting times t_w , experiment: Fig. 3

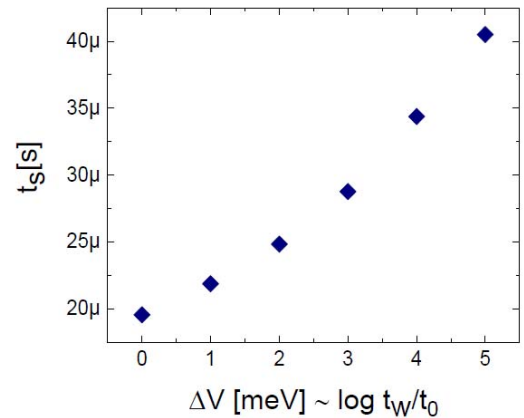


Fig. 15b. The increase of the switching time t_s with $\log t_w$, experiment: Fig. 4

To confirm the model new experiments are under investigation. The degree of crystallinity can be altered by the annealing temperature or by the preparation process. We find that with a higher degree of the crystalline phase or vice versa with a lower degree of the amorphous phase the magnitude of the imprint as well as the relaxational current is decreased. Results will be published soon.

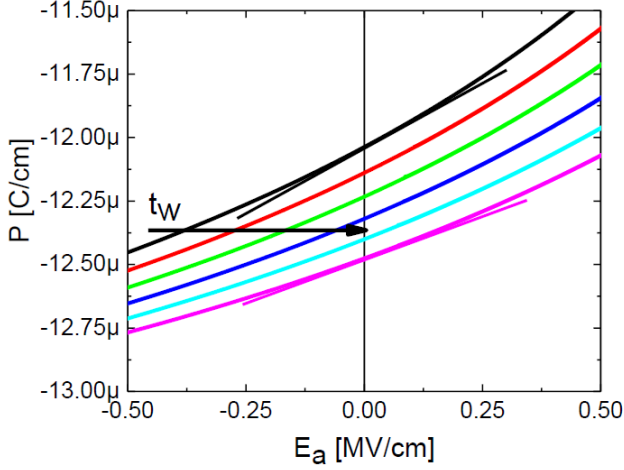


Fig. 16a. High resolution of the hysteresis loops in the negative remanent state (from Fig. 14a), box in Fig. 14a enlarged.

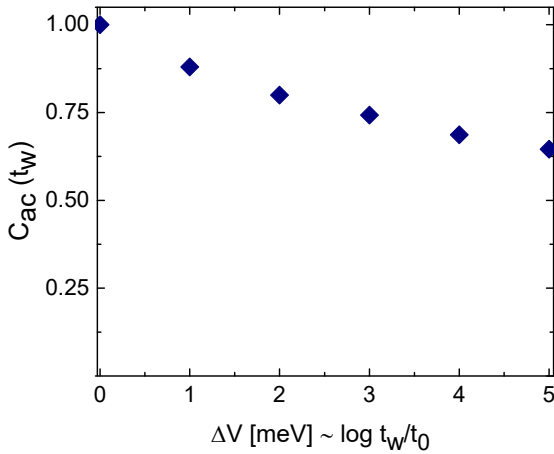


Fig. 16b. The calculated normalized capacitance depends on the waiting time, experiment: Fig. 5

IV. CONCLUSION

It is deduced how a feedback effect between the amorphous phase and the crystalline phase in a ferroelectric can lead to the imprint behaviour. To that at first appropriate models for the relaxational polarization of the amorphous phase and for the ferroelectric polarization of the crystalline phase are presented. In the amorphous phase charges/dipoles fluctuate in double well potentials which are not coupled among themselves. The dipoles/charges in the crystalline phase move also in double wells. Due to their crystalline order they are coupled to yield a ferroelectric state. The dipolar fields of the amorphous phase feed back into the neighbored crystalline phase. The ferroelectric polarization is stabilized due to the antiparallel alignment of the dipoles in the amorphous phase with respect to the alignment of the ferroelectric dipoles. The interaction is described by the

double well potential model: the dipolar fields of the amorphous phase reach into the crystalline phase and shift the double well potentials thus stabilizing the crystalline dipoles against reversal.

V. ACKNOWLEDGEMENT

Mr. Mag. rer. nat. Christian Peter co-developed the model of the imprint and he conducted the experiments regarding the imprint [20].

The author likes to thank Mr. B. Sc. Omar Elshehy for various model calculations. Dr. Andreas Leschhorn provided theoretical input and Mrs. Dr. Manfang Mai contributed basic experiments. Mr. M. Sc. Sujith Reddy Varakantham provided illustrations and Mrs. Nina Hort processed the manuscript.

VI. REFERENCES

- [1] C. Peter, A. Leschhorn, H. Kliem, "Characteristic time dependence of imprint properties in P(VDF-TrFE)" JAP **120**, 124105 (2016)
- [2] J. Lazareva, Y. Koval, P. Müller, K. Müller, K. Henkel, D. Schmeisser, "Interfacescreening and imprint in poly(vinylidene fluoride trifluoroethylene) ferroelectric field transistors" JAP **105**, 054110 (2009)
- [3] M. Grossmann, O. Lohse, D. Bolten, U. Boettger, R. Waser, "The interface screening model as origin of imprint in PbZr_xTi_{1-x}O₃ thin films. I. Dopant, illumination, and bias dependence" JAP **92**, 2680 (2002)
- [4] K. Carl, K.H. Haerdtl, "Electrical after-effects in Pb(Ti, Zr)O₃ ceramics" Ferroelectrics **17**, 473 (1977)
- [5] G. Arlt, H. Neumann, "Internal bias in ferroelectric ceramics: Origin and time dependence", Ferroelectrics **87**, 109 (1988)
- [6] J. Shi, H. Fan, X. Liu, Q. Li, "Defect-dipole alignment and strain memory effect in poled Li doped (Bi_{0.5}Na_{0.4}K_{0.1})_{0.98}Ce_{0.02}TiO₃ ceramics" J. Mater. Sc.: Mat. El., **26**, 9409 (2015)Y.
- [7] M. Mai, A. Leschhorn, H. Kliem, "The field and temperature dependence of hysteresis loops in P(VDF-FrFE) copolymer films", Phys. B: Condens. Matter **456**, 306 (2015)
- [8] M. Mai, "Polarization switching in ferroelectric films of P(VDF-TrFE) Copolymer", Dissertation Saarland University (2013)
- [9] B. Martin, M. Kuehn, H. Kliem, "Interacting and non-interacting dipole systems in ferroelectric poly(vinylidene fluoride-trifluoroethylene) copolymer", JAP **108**, 084109 (2010)
- [10] T. Guo, W. Guo, "A transient state theory of dielectric relaxation and some empirical laws", CEIDP Ann. Rep., 29 (1982)
- [11] K. J. Kim, N. M. Reynolds, S. L. Hsu, "Spectroscopic analysis of the crystalline and amorphous phases in a vinylidene fluoride/trifluoroethylene copolymer", Macromolecules **22** (1989)
- [12] H. Kliem, A. Leschhorn, "Modeling relaxor characteristics in systems of interacting dipoles", Physica B **503**, 167-173 (2016)
- [13] H. Kliem "Small signal response by protons in amorphous insulators" IEEE Trans, El. Ins. **24** 185 (1989)
- [14] L. Kankate, A. Gratsov, H. Kliem, "Nonlinear relaxational polarization in aluminumoxide", TDEI **22**, 1220 (2015)
- [15] H. Kliem, G. Arlt, "A relation between dielectric polarization currents and distribution functions", phys. stst. sol. (b) **117**, K 81 (1983)
- [16] H. Kliem "Untersuchungen zur dielektrischen Relaxation im Zeitbereich in Al₂O₃", Dissertation RWTH Aachen (1983)
- [17] P. Weiss "Sur la nature du champ moléculaire", Archives des sciences physiques et naturelles **37**, 201 (1914)
- [18] A. Leschhorn, H. Kliem "A feedback model for dielectrics, ferroelectrics and relaxors" CEIDP Ann. Rep. **89** (2016)
- [19] H. Kliem, A. Leschhorn, T. Edtbauer, "A model for the double loop of ferroelectric polarization close to T_c", JAP **113**, 104102 (2013)
- [20] Ch. Peter, H. Kliem "Feedback of the amorphous phase on the ferroelectric phase: Imprint effects in P(VDF-TrFE)", 2018 IEEE International Conference on Dielectrics (ICD), Budapest, accepted for the proceedings